

1 **Unpacking Tornado Disasters: Illustrating the Southeast U.S. Tornado-Mobile and Manufactured**
2 **Housing Problem Using the March 3, 2019 Beauregard-Smith Station, Alabama Tornado Event**

3 Stephen M. Strader^{1*}, David B. Roueche², and Brett M. Davis²

4 ¹*Villanova University, Department of Geography and the Environment*

5 ²*Auburn University, Department of Civil Engineering*

6 **Abstract**

7 This study illustrates and describes how Southeast U.S. tornado disasters commonly unfold by examining
8 the 2019 Beauregard-Smith Station, AL tornado event from spatiotemporal and structural engineering
9 stand points. Findings indicate that although the meteorological forecasts leading up to the tornado event
10 were accurate and timely, 23 individuals–19 in manufactured homes–still perished. All fatalities are
11 primarily a result of the lack of positive ground anchoring on homes where individuals were killed.
12 Altogether, the Beauregard-Smith Station, AL tornado event resulted in a housing fatality rate seven times
13 greater than the 2011 Joplin, MO EF5 tornado at least in part due to a disproportionately larger number of
14 manufactured homes exposed to violent tornado winds. Methods applied in this research should be
15 utilized by future studies documenting tornadoes so that patterns in structural failure mechanisms and
16 mortality can be determined. Integrated warning teams consisting of National Weather Service
17 forecasters, emergency managers, media partners, etc. and members of the manufactured housing industry
18 should work together using the results from this study to initiate a dialogue aimed at developing and
19 improving tornado disaster mitigation, response, and recovery strategies.

20
21
22 *Corresponding author address: Stephen M. Strader, Department of Geography and the Environment,
23 Villanova University, 800 E. Lancaster Ave., Mendel Hall G65F, Villanova, PA 19085, E-mail:

24 stephen.strader@villanova.edu

25 **Introduction and Background**

26 Tornadoes are one of the most costly and destructive hazards produced by severe convective
27 storms. Six of the ten costliest tornadoes on record have occurred since 2011, resulting in over 300
28 fatalities and 3,300 injuries (NCEI 2019). Approximately 70 people per year (30-year mean) are killed by
29 tornadoes, with most of these fatalities taking place in residential structures (Strader and Ashley 2018).
30 High-impact tornado events are most common in the Southeast U.S. where tornado casualty rates are
31 greatest due to a combination of factors such as a high percentage of housing stock that is mobile or
32 manufactured homes (**MH**), larger population and development density, elevated climatological tornado
33 risk, and more physically and socially vulnerable residents compared to other tornado-prone regions in
34 the U.S. (e.g., Ashley 2007; Sutter and Simmons 2010; Ash 2017; Strader and Ashley 2018).

35 *Tornado-mobile/manufactured housing problem*

36 There are two primary types of single-family residential structures, permanent home (**PH**) or MH.
37 Prior to 1976, any prefabricated (i.e., manufactured off-site) home constructed was deemed a “mobile
38 home”. In 1974, the U.S. Congress passed the Housing Construction and Safety Standards Act,
39 commonly called the Housing and Urban Development (**HUD**) code. The HUD code outlines and
40 describes minimum construction guidelines or standards for newly built prefabricated homes. In 1994,
41 HUD updated the code for MHs to significantly bolster design requirements in coastal areas—designated
42 Wind Zones II and III—with success (FEMA 2007; FEMA 2013 cf. their Figure G-1), but requirements
43 for Wind Zone I—non-hurricane prone regions of the U.S.—remained largely unchanged. As such, any
44 prefabricated home built after 1976 that follows the HUD code is referred to as a “manufactured home”.
45 There is not a significant difference between pre- and post-1994 MHs homes with respect to design
46 requirements in Wind Zone I. PHs are constructed in accordance with local building codes and designated
47 as either a site-built or modular home. A modular home is prefabricated and assembled on-site, while a
48 site-built home is constructed from materials on location.

49 From a physical vulnerability and structural quality perspective, MH structures are expected to

50 fail at wind loads less than 50% of those likely to destroy a PH (McDonald and Mehta 2004). As further
51 evidence of this enhanced MH wind vulnerability, 54% of all housing-related tornado fatalities take place
52 in MH structures although only 6% of the entire U.S. housing stock is made up of MHs (Strader and
53 Ashley 2018). Further escalating housing-related tornado fatality odds, many states within the Southeast
54 U.S. region contain MH housing stock percentages that are more than double that of the national average
55 (e.g., 13% Alabama, 14% Mississippi) according to Census data. Simultaneously, a majority of MHs in
56 the Southeast are located on isolated plots of land outside of city limits and not in MH communities or
57 parks (Strader and Ashley 2018). This MH development pattern is unique to the Southeast given a
58 majority of MHs in other regions such as the Midwest, Central Plains, Northeast, etc. are in urban or
59 suburban density MH parks or communities.

60 MH residents are also more likely to be socioeconomically vulnerable to tornado impacts since
61 they regularly fall into one or several vulnerability-enhancing categories such as having a lower
62 household income, relying on public assistance, being disabled, etc. (Cutter et al. 2012; Ash 2017; Ash et
63 al. 2020; Rumbach et al. 2020). Together, the greater number of less wind resistant housing structures,
64 elevated socioeconomic vulnerability, and a larger percentage of MHs in rural or exurban areas in the
65 Southeast elevates tornado impact and disaster potential within the region (Strader and Ashley 2018).

66 *Post-event tornado damage surveys*

67 The first step in determining tornado impact severity and magnitude after an event is to conduct a
68 rapid, post-mortem analysis based on initial reports from first responders, affected populations, etc.
69 Following this initial assessment, an in-person, post-event damage survey is routinely conducted by a
70 local National Weather Service (NWS) forecast office for the purpose of gathering information about the
71 tornado's wind speeds, path length, maximum path width, damage magnitude, etc. (Marshall 2002;
72 Prevatt et al. 2012b; Roueche and Prevatt 2013; Strader et al. 2014; Roueche et al. 2017). In high impact
73 events, it is also common for additional or complementary survey teams consisting of wind and structural
74 engineers from academia, private industry, and government agencies to operate in parallel or assist the

75 NWS with data collection (Prevatt et al. 2012a; Roueche and Prevatt 2013). These additional post-event
76 damage assessments have proven useful for enhancing official NWS surveys by obtaining fine-scale
77 details or information related to tornado damage indicators (**DI**), degree of damage (**DOD**), tornadic wind
78 field characteristics, etc. (Prevatt et al. 2012a; Roueche and Prevatt 2013; Burgess et al. 2014; Kuligowski
79 et al. 2014; Lombardo et al. 2015; Egnew et al. 2018; Ree and Lombardo 2018).

80 A principal objective of this study is to illustrate how Southeast U.S. tornado disasters commonly
81 unfold at the local scale and lead to fatalities due to the combination of a significant (Enhanced Fujita
82 scale; EF2+) or violent (EF4+) tornado intersecting vulnerable MH residents. This study also
83 demonstrates how high-resolution MH location data, fine-scale built-environment, land use-land cover
84 (**LULC**) data can be combined with Doppler radar products in near real-time (i.e., as the tornado is still
85 on the ground or within one hour after the tornado impacts a region) to estimate potential tornado impacts
86 on the underlying landscape. Although prior research has illustrated that socioeconomic and demographic
87 population characteristics play a role in tornado disaster severity, we do not assess or quantify these
88 variables during the tornado Beauregard-Smith Station, AL tornado event because of the difficulty of
89 acquiring fine-scale and accurate data linked to those that survived and/or were killed in the event.
90 Nevertheless, the Beauregard-Smith Station, AL tornado event is used as an exemplar for informing and
91 applying near real-time geospatial analyses within rapid, structure-by-structure tornado damage
92 assessments to generate a more holistic, comprehensive, and thorough understanding of how tornadoes
93 and elevated MH density in the Southeast U.S. often lead to fatalities and disaster.

94 **Data and Methodology**

95 *3 March 2019 severe weather conditions and Doppler radar data*

96 To provide a detailed meteorological overview of the 3 March 2019 event, we first examined
97 forecast discussions and products issued by the NWS and Storm Prediction Center (**SPC**) in the days and
98 hours prior to the severe weather event. Additional tornado warning information was gathered from the
99 Iowa Environmental Mesonet (**IEM**) storm warning verification tool to assess warning lead time for

100 populations in Macon and Lee counties. Doppler radar base reflectivity, storm relative velocity, and
101 correlation coefficient data from KMXX in southeastern Alabama were employed to illustrate the
102 potential tornado damage path and intensity (NWS 2019a). Complementary Multi-Radar/Multi-Sensor
103 System (**MRMS**) rotation track data were also gathered to assist the raw Doppler radar data in
104 determining a *potential* tornado damage area of interest (**AOI**) in near real-time (NSSL 2019).

105 *Built environment and LULC data*

106 A combination of fine-scale building footprint, land parcel, housing, critical infrastructure, and
107 LULC data were employed to estimate potential tornado impacts in near real-time. Microsoft's US
108 Building Footprints dataset was acquired to determine the number of structures (e.g., homes, public
109 buildings, commercial buildings, barns, garages, sheds) that might have been damaged by the tornado
110 (Microsoft 2018). Additional built-environment entities such as homes, retail stores, restaurants, gas
111 stations, office buildings, manufacturing/storage facilities, etc. were derived from county land-parcel data
112 acquired prior to the event. Lastly, MH location data from Strader and Ashley (2018) were employed to
113 provide a more complete and accurate representation of MH locations across Alabama.

114 In addition, Homeland Infrastructure Foundation-Level Data (**HIFLD**) were used in conjunction
115 with land-parcel data to determine whether important or critical community, state, or federal structures
116 were affected by the tornado (Homeland Security 2020). The National Land Cover Database (**NLCD**)
117 2016 was also utilized to determine the types of LULC likely damaged in the tornado path (Wickham et
118 al. 2014). The NLCD dataset comprises 15 LULC classifications including four classes of developed land
119 area (open, low, medium, and high intensity development). A supplemental land use dataset (Spatially
120 Explicit Regional Growth Model; **SERGoM**) was used in conjunction with the NLCD LULC data to
121 estimate housing density within the potential tornado damage path (Theobald 2005). Housing unit density
122 is broken down into four classes: urban (<0.1 ha per home), suburban (0.1–0.68 ha per home), exurban
123 (0.68-16.18 ha per home), and rural (>16.18 ha per home).

124 *Post-event damage survey data collected*

125 Tornado damage information following the 3 March 2019 Beauregard-Smith Station tornado was
 126 collected using hands-on, door-to-door damage surveying techniques, drive-by damage assessments,
 127 targeted use of unmanned aerial systems (UAS), aerial imagery of the entire track captured from a low-
 128 flying aircraft, and synthesis of supplemental data sources (e.g., county property assessor information,
 129 pre-event and post-event Street view imagery hosted through Google Street View). Door-to-door damage
 130 observations were documented using the Fulcrum data collection platform from spatialnetworks.com,
 131 which uses a smartphone application to attach photographs and other media to a geolocated survey form.
 132 The survey forms applied in this study included a general building assessment sheet developed by the
 133 Structural Extreme Events Reconnaissance network (StEER; Kijewski et al. 2018), and a form
 134 specifically focused on MHs to allow for more precise details regarding anchorage, presence of corrosion,
 135 pier height variations, and other critical construction and installation parameters to be collected in a
 136 standardized format.

137 Damage assessments documented the precise location, building attributes, structural load path,
 138 and observable damage, if present. Damage to buildings was assessed using the DODs in the EF Scale
 139 and the StEER wind damage ratings, which categorize physical damage with emphasis on resulting
 140 economic losses (Vickery et al. 2006). The assessments were further categorized by building type using
 141 the DIs of the EF Scale. The commonly observed DIs (i.e., building types), were 1- and 2-family
 142 residences (DI2), single-wide MHs (SWMH; DI3), and double-wide MHs (DWMH; DI4), each of which
 143 have different DODs (i.e., progressive descriptions of damage unique to each DI) associated with them.
 144 To facilitate comparisons between these DIs in analyses, a Degree of Damage Index (DODi) was
 145 developed and utilized to normalize the DODs for each DI. The DODi is defined as follows:

$$146 \quad DODi(di, dod) = \frac{(WS_{di,dod} - WS_{di,DOD_1})}{(WS_{di,DOD_{max}} - WS_{di,DOD_1})}$$

147 where $WS_{di,dod}$ is the expected wind speed for an observed DOD to a given DI, WS_{di,DOD_1} equals the
 148 expected wind speed for DOD1 (i.e., the threshold of visible damage for each DI), and $WS_{di,DOD_{max}}$ is
 149 the expected wind speed associated with the highest DOD for the given DI. Thus, the DODi normalizes

150 the damage in a 0-1 scale across all DIs, with 0 being the threshold of visible damage and 1 representing
151 the highest damage state. For DIs 2, 3, and 4, $DOD_i = 1$ represents complete destruction with debris
152 swept away from site for typical buildings. Further, the employed StEER wind damage ratings were
153 modified to better separate economic destruction (i.e., structure is a total loss and must be replaced) from
154 life-safety destruction (i.e., structure failed in such a way that life-safety was put at risk). The original
155 wind damage ratings are “No Damage”, “Minor”, “Moderate”, “Severe”, and “Destruction”. In the
156 modified wind damage ratings, “Destruction” is split into two separate ratings, with Destruction (“High
157 Risk”) representing any buildings in which all walls were collapsed—which also included lofting or
158 rolling of MHs, and Destruction (“Low Risk”) representing structural failures which resulted in total loss
159 economically, but were a low life-safety risk due to walls and even portions of the roof still intact to
160 provide resident shelter.

161 Most buildings with considerable structural damage were investigated on-site between 4 March
162 2019 and 13 March 2019 by a team of two wind/structural engineers, while buildings in the outer regions
163 of the tornado with minor or no damage were generally investigated via drive-by assessments and
164 UAS/aerial imagery within the same time period again by a team of two wind/structural engineers.
165 Supplementary information such as photographs and narratives available from the NWS Damage
166 Assessment Toolkit were used to augment the damage assessments when and where available. The
167 tornado damage survey team placed an emphasis on collecting fine-scale and detailed information related
168 to the structural performance of each home where a fatality occurred. Precise fatality locations were
169 obtained using a variety of sources such as public media reports, social media posts related to the victims,
170 and public tax assessor records.

171 In total, the post-event damage assessment documented the structural performance of 769
172 structures within the Alabama portion of the tornado damage path. Initial assessment targets were
173 informed by the fine-scale MH dataset and geospatial assessments discussed in the above sections. The
174 ensuing assessments included 474 (62%) PHs, 229 (30%) MHs, and 64 (8%) other structures falling

175 within a variety of classifications (including sheds and outbuildings), which included five churches, and
176 four buildings on the West Smith Station Elementary campus.

177 Overall, the study results are split into four primary sections (**Figure 1**). Results section (1)
178 provides a summary and temporal perspective on the meteorological conditions, forecast performance,
179 and tornado warning lead times prior to the Beauregard-Smith Station tornado (**Figure 1**; green boxes).
180 Results section (2) outlines and describes geospatial assessments of potential tornado impacts on the
181 underlying landscape in near-real time and immediately following the tornado event (**Figure 1**; yellow
182 boxes). The analyses conducted in section two of the results were also designed to inform the rapid, in-
183 person, post-event tornado damage survey conducted in the days and weeks following the tornado.
184 Section (3) of the results provides an overview of the structural performance of buildings in the damage
185 path using fine-scale tornado damage survey techniques (**Figure 1**; red boxes). Lastly, results in section
186 (4) concentrates on those locations, circumstances, damage findings, etc. where fatalities occurred
187 (**Figure 1**; blue boxes).

188 **Results**

189 *Meteorological conditions, forecast performance, and warning lead times*

190 On 1 March 2019, the SPC released their Day 3 categorical and probabilistic severe weather
191 outlooks, indicating a slight risk (15%) for the Southeast U.S. (**Figure 2A**). While this initial forecast did
192 mention the potential of a few tornadoes, the primary concern were storms that could produce straight-
193 line winds, not rotating storms (e.g., supercells). Severe weather probabilities were amplified in the Day 2
194 SPC convective outlook released the day before the tornado event, increasing the probabilistic and
195 categorical risk from 15% (slight) to 30% (enhanced) for areas of southeastern Alabama (**Figure 2B and**
196 **C**). The primary forecast concern in the Day 2 outlook was the increasing likelihood of discrete
197 supercells. For the Day 1 SPC outlook, severe weather probabilities were decreased from 30% to 10%.
198 This reduction in severe weather potential was again due to concerns about a more dominant straight-line
199 wind producing storm mode (i.e., quasi-linear convective system) that would be less favorable for tornado

200 production (**Figure 2D and E**). Similar to the Day 2 convective outlook, the Day 1 outlook noted that
201 rotating storms and strong tornadoes would be possible where there would be a collocation of moderate
202 instability ($500\text{-}1500\text{ J kg}^{-1}$), high surface moisture (dew point temperatures of 15 C (60 F)), and strong
203 low-level shear (50-70 kts) in the warm sector of the synoptic system.

204 At 15:59 UTC (9:59 AM CST) on 3 March 2019, the SPC issued their first mesoscale discussion
205 (**MD**) for portions of southeastern Alabama (**Figure 2F**). This MD was released approximately two hours
206 prior to the first tornado watch that covered the same region. The primary MD concern was the initial
207 signs of discrete convection starting to develop in the warm sector where previous SPC outlooks had
208 suggested some strong tornadoes could occur in southeastern Alabama. A second MD issued by the SPC
209 at 18:02 UTC (12:02 PM CST) for portions of southeastern Alabama mentioned the amplifying likelihood
210 for discrete supercell development and subsequent tornadoes over the next two hours (**Figure 2G**).

211 Approximately an hour later, a third MD encompassing Macon and Lee counties was released based on
212 radar imagery indicating a maturing supercell moving into an area that would be supportive of rotating
213 thunderstorms and tornadoes (**Figure 2H**). In fact, the MD stated, “*Given the ample buoyancy and intense*
214 *shear profile in place, it appears tornadogenesis will likely occur within the next 30-60 minutes with the*
215 *possibility of a strong tornado occurring.*” After the Bearegard-Smith Station tornado formed, a final
216 MD was issued at 20:19 UTC (2:19 PM CST) indicating that there was a high probability the outlined
217 region could experience wind speeds of 125-175 mph (**Figure 2I**).

218 The NWS Birmingham, AL weather forecast office issued the first tornado warning for the
219 Bearegard-Smith Station, AL tornado at 19:19 UTC (1:19 PM CST). This warning yielded a 41-minute
220 lead time for those in far eastern Macon county where tornadogenesis eventually occurred. A second
221 tornado warning was issued for Lee County at 19:58 UTC (1:58 PM CST) just prior to the
222 tornadogenesis. The tornado warning for Lee County provided a lead time of approximately five minutes
223 for the southwestern areas in Lee County and a 32-minute lead time for eastern county portions. The
224 location where most tornado fatalities occurred (i.e., Route 38 and Highway 51 in Lee County) received
225 approximately nine minutes of tornado lead time, which is less than the national average of approximately

226 15 minutes (Brooks and Correia 2018). Nevertheless, the SPC and NWS forecast was consistent and
227 informative, providing Alabama residents with ample time to plan, prepare, and react to any severe
228 weather threats. Yet, 23 individuals were killed, suggesting that other factors such as tornado intensity,
229 population and built-environment exposure, building structural integrity, etc. played a more critical and
230 vital role during the event.

231 *Assessing potential impacts in near-real time using radar, built-environment, and LULC data prior to the*
232 *rapid tornado damage survey*

233 i. Potential impact assessment: Doppler radar products

234 As the tornado event unfolded and immediately after the tornado was confirmed to be on the
235 ground, we acquired a variety of raw and derived Doppler radar products covering Macon and Lee
236 counties. There were five Doppler radar scans of the tornadic supercell made between tornadogenesis and
237 prior to the tornado crossing the Alabama-Georgia state line (**Figure 3A**). The first Doppler radar base
238 scan (0.5 degrees; lowest tilt) intersected the mesocyclone portion of the supercell in eastern Macon
239 County at approximately 300 m (1,000 ft) above ground level (**AGL**). As the storm and tornado moved
240 east-north easterly, a final base-level radar scan intersected the mesocyclone region of the supercell at 860
241 m (2,820 ft) AGL. The KMXX lowest-level radar tilt data were deemed sufficient for remotely
242 determining the potential tornado damage path and assessing possible societal impacts prior to the in-
243 person damage survey to be conducted on the following day because the radar was likely sampling the
244 low-level mesocyclone portion of the storm responsible for the ongoing tornado.

245 The base reflectivity radar data illustrated a well-defined mesocyclone or hook echo on each scan
246 from 20:01 UTC to 20:27 UTC. High base reflectivity returns of greater than 60 dBZ were also apparent
247 in the hook echo region of the supercell at 20:07 UTC, highlighting a tornado debris signature (**TDS**;
248 **Figure 3A**; Bodine et al. 2013; Van Den Broeke 2014). Storm relative velocity data from the 20:07 UTC
249 scan denoted a maximum rotational velocity of 57 kts (**Figure 3B**). This rotational velocity magnitude is
250 consistent with prior research that has determined that rotational velocity values of 55 to 75 kts are

251 commonly associated with significant tornadoes (Smith et al. 2015; Thompson et al. 2017; Gibbs and
252 Bowers 2019). Correlation coefficient values less than 0.5 were also evident from 20:07 UTC to 20:27
253 UTC in the mesocyclone or updraft portion of the storm (**Figure 3C**). Radar scan tilts above base level
254 illustrated correlation coefficient values consistent with debris being lofted by a significant tornado up to
255 5 km (16,400 ft; Kingfield and LaDue 2015). The MRMS rotation track denoted strong azimuthal shear
256 values upwards of 0.02 s^{-1} across Lee County (**Figure 3D**). Together, the base reflectivity, velocity,
257 correlation coefficient, and rotation track data all indicated that it was likely that a significant or violent
258 tornado traversed eastern Macon and southern Lee County from approximately 20:00 UTC to 20:30 UTC
259 causing substantial damage to the underlying landscape.

260 ii. Potential impact assessment: Built environment and LULC

261 A potential damage area of interest (**AOI**) based on the KMXX Doppler radar scans on 3 March
262 2019 from 20:01 UTC to 20:27 UTC was generated to assess potential built- and natural-environment
263 impacts prior to the in-person damage assessment (**Figure 3**). This AOI was intentionally designed to
264 overestimate the tornado damage path so that it would represent a high-end impact estimate for the event.
265 High-end impact estimates provide emergency managers and first responders with a “worst-case
266 scenario” so that they can be best prepared to respond to any disaster situation (Clarke 2005). Based on
267 the potential damage AOI, there were 2,791 buildings possibly damaged by the tornado. Approximately
268 67% of the buildings in the AOI were PHs or MHs, with 37% (1,020) being PHs. MHs represented 30%
269 (852) of all AOI building footprints and made up nearly 45% of all homes. This percentage of MH
270 housing types is nearly 3.6 times greater than the Alabama state percentage of MH housing stock (13%;
271 Census 2020). There were also six MH parks or communities in the potential damage AOI, with each of
272 them containing less than 50 MH individual units. In addition to homes, there were approximately 44
273 other buildings within the AOI as well. These 44 buildings included churches, retail stores, gas stations or
274 convenience stores, warehouses or manufacturing businesses, fire stations or emergency medical services,
275 and an elementary/secondary school. Aside from buildings, there were 133 different roads, two high-

276 tension power line regions, and a cell phone tower within the AOI. However, potential impact analyses
277 also denoted that buildings such as federal, state, or local buildings, hospitals, university/college-related
278 properties, etc. were not exposed to tornadic winds and subsequently damaged.

279 An estimated 84.1 km² (60%) of the AOI was estimated to be forested LULC, with evergreen
280 forests representing the largest percentage of forested area at 23.3%. An additional 47.8 km² (34%) of the
281 potential tornado damage AOI comprised natural and agricultural lands. Only 8.4 km² (6%) of the AOI
282 region was considered developed LULC, with most (5.1 km²) of the development being classified as open
283 development (i.e., less than 20% impervious surfaces with development being situated within mostly
284 open areas and mixed vegetation). The SERGoM housing unit densities support this development
285 character given 96.3% of the potentially affected landscape was considered rural or exurban land use
286 density. A majority 60% of the area underneath of the AOI was considered exurban density. Only 1.1% of
287 the exposed landscape was suburban or urban. Overall, the LULC and developed/housing unit density
288 analyses indicate that the tornado may have crossed a largely undeveloped landscape where most homes
289 in the region were in exurban density.

290 *Rapid in-person, post-event damage assessment*

291 The Beauregard-Smith Station tornado was rated an EF4 with an estimated maximum wind speed
292 of 170 mph (NWS 2019b). Tornadogenesis occurred at 20:00 UTC (2:00 PM CST) near Society Hill, AL.
293 and continued east-northeast at approximately 60 mph. The tornado path length in Alabama was 44 km
294 (27 mile) with a maximum path width of 1.5 km (1 mile). The tornado crossed the Alabama-Georgia state
295 line at 20:29 UTC (2:29 PM CST) near Smith Station, AL. Overall, the tornado resulted in 23 fatalities
296 and over 90 injuries, with most injuries occurring in the corridor from Lee Rd 36 to Lee Rd 38 in Lee
297 County (**Figure 4**). The locations of the fatalities and injuries aligned with the areas in which the most
298 significant damage occurred, which was primarily in the first 20 km (12 miles) following tornadogenesis.
299 The observed damage and MRMS data indicate the tornado decreased in intensity as it moved towards
300 Smith Station and across the Alabama-Georgia border. The rapid post-event assessment identified a

301 spectrum of performance across the various building typologies, primarily single-family homes (both PHs
302 and MHs). A total of 380 buildings and other structures experienced visible exterior damage out of the
303 769 that could reasonably be assumed to have been affected by the tornado. The count of damaged
304 buildings included 174 permanent homes (PHs; site-built or modular), 49 SWMHs, 105 DWMHs, 40
305 barns, sheds or similar buildings, and 12 non-residential buildings. MHs comprised 47% of all residential
306 structures that received visible exterior damage. SWMHs and DWMHs represented 15% and 32% of all
307 homes damaged in the tornado, respectively. Nearly, 70% of the MHs affected by the tornado were
308 DWMHs as well. Together, these findings indicate that a disproportionately large percentage of MHs
309 were exposed to the tornadic winds compared to the surrounding region (i.e., only 13% of the entire
310 Alabama housing stock is made up of MHs).

311 The average (mean) year of construction for all buildings with visible damage was 1986, with
312 means of 1984, 1994 and 1994 respectively for PHs, SWMHs and DWMHs. The on-site, post-event
313 tornado damage investigation found that construction quality within the path was generally poor to
314 average, with no evidence of enhanced wind-resistance construction (e.g., metal strap roof-to-wall
315 connections, oversized anchor bolt washers, structural wall sheathing throughout) in the vast majority of
316 affected buildings. Specific to MHs, the investigation noted the common use of pan anchorage systems in
317 lieu of traditional tie-down straps and ground anchors in newer MHs. These pan systems consisted of
318 diagonal struts that transferred lateral loads to a metal pan that rests on the ground. The weight of the
319 home is relied upon to both resist all uplift forces, and provide sufficient gravity loads to create the static
320 friction between the pan and the soil necessary to resist design lateral loads.

321 Wind performance for all buildings was primarily a function of distance along the length of the
322 tornado damage path, distance from the centerline of the tornado (as estimated by the NWS (NWS 2019
323 b) damage path, approximate center of heaviest damage, and building typology (**Figure 5**)). Observations
324 indicated that robustness of the foundation or anchorage system played a significant role in determining a
325 building's wind performance and/or damage severity within the tornado path. Although building
326 orientation was a factor for all building types, the damage survey indicated that it was most important for

327 MHs (Roueché et al. 2019). Significant damage to non-residential structures was limited to older
328 commercial and religious facilities with light-frame wood or unreinforced masonry structural systems.
329 The most severe damage to non-residential buildings was experienced by a small, unreinforced masonry
330 church located near the beginning of the tornado path that was destroyed. No non-residential structures
331 were located within the path of the tornado when its intensity was the highest, near HWY 51 and Lee Rd
332 38. Non-residential structures were more common in and around Smith's Station, where intensity of the
333 tornado was reduced, and damage was very minor outside of a car dealership and restaurant. Both the car
334 dealership and restaurant were older (pre-2000) light wood-frame buildings that experienced loss of the
335 structural roof system. The only school affected within the tornado path was the West Smith Station
336 Elementary School, which experienced minor cladding damage, collapse of a few exterior covered
337 walkway structures, and loss of some rooftop HVAC equipment. The tornado also induced the collapse of
338 a cellular tower in Smith Station near US 280.

339 Of the 380 structures affected by the tornado, 328 were single-family homes (DIs 2, 3 and 4 in the
340 EF Scale). To better assess tornado impact severity to these structures, the tornado damage path was split
341 into two primary geographic components, Region A and Region B (**Figure 5**). The tornado path was split
342 into these two regions based on damage severity and potential changes in tornado intensity as discussed
343 previously. Damage was more severe within the first 20 km (12 miles) of the tornado path (designated
344 Region A) than in the remainder of the path (designated Region B). Within Region A, complete structural
345 failure in both PHs and MHs was most common within an approximately 250 m buffer on each side of the
346 tornado centerline. Within this region, and in general across the entire tornado width in Region A,
347 SWMHs sustained the highest damage on average, with PHs sustaining the lowest damage on average
348 (**Figure 5B, D**). In Region B, extending from the edge of Region A to the Alabama-Georgia border,
349 complete structural failure rarely occurred, despite similar building typologies, indicating the reduction in
350 tornado intensity (**Figure 5C, D**). In both regions, SWMHs were the most likely to exhibit complete or
351 catastrophic failure (**Figure 6**), with 54% in region A, and 13% in Region B, exhibiting damage with a
352 high risk to life-safety. This corresponded to 22 of the 41 damaged SWMHs in Region A, and one of the

353 eight damaged in Region B, that experienced DOD6 or higher (i.e., the unit rolled, lofted, and/or
354 experienced the destruction of the roof and all walls). DWMHs and PHs demonstrated better
355 performance, with 29% (20 out of 70) of DWMHs and 16% (8 out of 50) of PHs with failures deemed
356 high risk to life-safety in Region A, and 0% (0 out of 35) and 2% (2 out of 124) respectively in Region B.
357 The two high risk PH failures in Region B occurred in a section of poorly constructed, low-income homes
358 in Smith Station.

359 The *key failure mechanism* that led to the destruction of several PHs and many MHs *was the*
360 *lack of any positive anchorage to the ground*. Many PHs were simply resting on unreinforced masonry
361 stem walls that offered no resistance to the uplift forces induced by a tornado, a weakness recognized in
362 past studies also (e.g., Marshall 1993; Prevatt et al. 2012a). Where PHs were constructed on concrete
363 slabs, with anchor bolts to the slab through the sill plates, at a minimum some walls were always left
364 standing even with complete destruction of surrounding buildings. In MHs, previous studies have linked
365 destruction with the lack of anchorage altogether (e.g., Kensler 1985; Sparks 1985), but in this study, all
366 observed MHs appeared to have some anchorage/stabilizing system present at time of tornado impact.
367 However, the use of alternative pan anchorage systems, which rely upon the self-weight of the structure to
368 resist any uplift forces, and the frequent corrosion of ground anchors and diagonal straps where used,
369 compromised the wind resistance of these homes, potentially allowing catastrophic failures to occur at
370 relatively low wind speeds (**Figure 7**). For example, in several cases, the debris from a MH revealed that
371 the home failed due to the radial inflow of the oncoming tornado, pulling the structure towards the
372 tornado as it was destroyed. This complete destruction therefore occurred prior to when the tornado's
373 most intense winds could impact the MH.

374 A considerable trend in the MH failures was the overall lack of an optimum damage progression.
375 While damage generally initiated with loss of roof cover and cladding elements, very rarely was the loss
376 of roof sheathing or roof structure observed with the anchorage system intact. The four primary
377 mechanisms of structural failures observed in MHs consisted of the following: 1) separation at the
378 marriage line (DWMHs only), 2) roof-to-wall connection, 3) wall-to-floor connections, and 4) failure of

379 the anchorage system resulting in either sliding, overturning, or lofting (**Figure 8**). Of these potential
380 mechanisms, the anchorage system was nearly universally the first element of the structural load path to
381 fail during the tornado, compromising the entire structure and the safety of the occupants. This lack of
382 “safe” failures in both SWMHs and DWMHs relative to PHs is exemplified in **Figure 6**. Specifically, 12
383 of the 20 destroyed PHs in Region A were deemed low risk failures in that at the very least some walls
384 were left standing although the home was a total loss. In contrast, only 1 of the 23 destroyed SWMHs and
385 3 of the 23 destroyed DWMHs could be considered low risk failures. Conversely, the remaining 19 MHs
386 were destroyed with nothing left in their original locations as determined by the combination of the debris
387 swaths, MH location data, and local parcel or tax records. The implications of this finding within the
388 context of the fatalities that occurred are discussed later in this article.

389 *Potential tornado damage AOI and actual post-event, damage survey impact differences*

390 As illustrated in the prior section, there were some differences between the real-time estimated
391 tornado impact and post-event damage assessments. To determine the actual number of structures,
392 facilities of interest, LULC percentages, etc. affected by the Beauregard-Smith Station tornado, a
393 combination of the post-event tornado damage assessment and the NWS post-event surveyed tornado
394 damage polygon was used. Given the coarse spatial resolution of the KMXX Doppler radar data, the
395 potential tornado damage AOI overestimated the total impact on the underlying landscape. This finding
396 was expected given the AOI represented a potential damage area of 140 km² compared to an actual
397 damage path area of approximately 40 km² based on the NWS-surveyed damage path. The larger
398 potential tornado AOI compared to the actual damage path meant that some of the structures thought to be
399 exposed in the tornado were not damaged. For example, none of the six MH parks, EMS/fire stations,
400 manufacturing/warehouses, or office buildings sustained any visible tornado damage based on the post-
401 event damage assessment. Although 12 churches were thought to be potentially struck by the tornado,
402 only one received damage near the beginning of the tornado damage path.

403 Nevertheless, the near-real time estimates of tornado damage using the AOI performed
404 reasonably well. Doppler radar raw and derived products indicated that there was indeed a significant-to-
405 violent tornado on the ground in southern Lee County, while the housing data suggested that large
406 number of MHs were potentially in the violent tornado’s path. Further, LULC data illustrated that most of
407 the MHs were not in MH communities, but rather in exurban or rural land use densities. The restaurant,
408 car dealership, elementary school, and cell phone tower were all expected to have sustained damage based
409 on the near-real time assessment and did so based on the post-event damage survey.

410 In general, the near-real time provided immediate insight on potential tornado intensity and
411 impacts. This type of analysis not only helped determine the severity of tornado impacts in real time, but
412 also provided much needed information for subsequent in-person, post-event assessments conducted in
413 the days and weeks after. Not only will similar analyses be conducted for future potential high-impact
414 tornado events, additional modeling and analysis techniques will be added to the methodology so that
415 damage estimation techniques can be improved. The ultimate goal of future work using this technique
416 should be to provide a tool and methodology for NWS forecasters, emergency managers, first responders,
417 and critical personnel to better estimate potential real-time tornado impacts on vulnerable populations.

418 *Event fatalities, circumstances, and structural performance*

419 In all, 19 of the 23 (82.6%) Beaugard-Smith Station tornado fatalities transpired in MHs
420 (Roueché et al. 2019), and all fatalities occurred in homes that the post-tornado event survey identified as
421 high-risk failures. Fatalities occurred in 2 of the 8 PHs, 4 of the 23 SWMHs, and 8 of the 23 DWMHs that
422 were deemed high-risk failures. Anchorage systems in these MHs were observed to be either pan systems
423 or tie-down straps and ground anchors, but the precise details for each home’s anchorage (e.g., number of
424 anchors and connection details) could not always be discerned due to shifting or removal of the debris by
425 first responders. Both PHs where victims were killed were wood-frame homes constructed atop
426 unreinforced masonry stem walls with a crawl space. No positive attachment to the stem wall or interior
427 piers was observed in these two PHs. Structurally, PHs constructed in this way—which is common across

428 the Southeast—are similar to MHs in that they rely upon the weight of the home to resist uplift and, to an
429 extent, sliding wind loads. While a PH will generally have a higher self-weight than a MH due to the
430 larger structural member sizes used, any effects of this weight difference were not witnessed during the
431 post-event damage assessment. Thus, it is apparent that the two PHs where fatalities transpired performed
432 similar to MHs within the same region.

433 Based on the total number of homes observed with visible exterior damage, the tornado
434 encompassed a fatality rate of 7 fatalities per 100 homes for all housing types (**Table 1**). This fatality rate
435 is nearly *seven times greater* than the fatality rate associated with the 22 May 2011 Joplin, MO EF5
436 tornado where 80 residential fatalities occurred in 7,411 damaged homes (Kuligowski et al. 2014). The
437 primary difference between these two disasters is the total number of MHs affected in each event. For
438 instance, none of the 161 deaths in the Joplin, MO tornado transpired in MHs (Kuligowski et al. 2014;
439 Paul and Stimers 2014), and none or very few MHs were noted to have been impacted by the tornado.
440 Yet, 19 of 23 fatalities in the Beaugard-Smith Station, AL tornado were in MHs. As discussed prior,
441 most homes in the Beaugard-Smith Station tornado failed closer to the base of the superstructure (e.g.,
442 wall-to-floor connection, anchoring system), subjecting the occupants to wind-blown debris and blunt-
443 force trauma (**Figure 8**). The fatality rate in MHs was 12 fatalities per 100 MHs damaged (11.3 and 14.0
444 for DWMHs and SWMHs). This fatality rate is 5.3 times higher compared to the number of fatalities per
445 100 PHs damaged in the Beaugard-Smith Station tornado.

446 Together, these findings illustrate that a primary cause of the high fatality rates in the Beaugard-
447 Smith Station, AL EF4 tornado was the elevated number of MHs, which provide minimal (with tie-down
448 straps and ground anchor systems) or no (with alternative pan systems) positive anchoring to protect
449 against wind-induced uplift forces that exceed the self-weight of the home. Each of the MH-tornado
450 fatalities in Lee County also transpired in MHs built after 1983, suggesting that these structures were
451 more susceptible to complete destruction compared to PHs despite being constructed under post-1976
452 HUD code construction standards. The mean age of MHs where fatalities occurred was 20 years old,
453 where construction years ranged from 1983 to 2007. Fatality rates were similar across both MH types,

454 with 12 of the 19 MH fatalities occurring in DWMH structures, compared to seven in SWMHs.
455 Unfortunately, a common theme witnessed throughout the in-person damage survey was the lack of
456 positive anchorage in both older site-built homes where fatalities occurred as well. This finding suggests
457 that regardless of housing type and age, homes with no positive anchorage to resist uplift forces are at
458 much higher risk of incurring fatalities in violent tornadoes. Our hypothesis is that in a high wind event,
459 these housing types sustain a structurally brittle failure (i.e., sudden, with little to no inelastic deformation
460 prior to failure and thus little to no energy dissipation) at the foundation that prematurely compromise the
461 integrity of the remaining structure and enhances the probability of occupants being killed or seriously
462 injured. More detailed analysis of the tornado wind field is being conducted to evaluate at what wind
463 speeds such destruction is likely, but the analysis is outside of the scope of this paper.

464 All Beauregard-Smith Station tornado fatalities occurred in the first 20 km of the damage path
465 where tornado lead time was approximately 9 to 12 minutes. The lack of fatalities in the remaining
466 portions of the tornado path is likely due to the tornado weakening in intensity (resulting in fewer high
467 risk structural failures) in combination with the advanced warning from the NWS (i.e., tornado
468 emergency warning) and the prior storm history that allowed those affected to better prepare for the
469 tornado and seek shelter.

470 The portion of the tornado path where most (13 of 14 homes) fatalities were located was
471 considered largely exurban land use density. And, as mentioned prior, the tornado did not strike any MH
472 parks or communities. As discussed in Strader and Ashley (2018), nearly 80% of MHs in Alabama are not
473 in MH parks, but rather exurban and rural land use. The more dispersed MH density makes it more likely
474 that Alabama MHs are struck by a given tornado. Thus, the Beauregard-Smith Station, AL tornado is a
475 prime example of the MH-tornado relationship that frequently plagues the Southeast U.S.

476 **Conclusions**

477 This study employed an interscience approach to investigate the 3 March 2019 Beauregard-Smith
478 Station, AL EF4 tornado event. The research encompassed two primary goals: 1) illustrate how Southeast

479 U.S. tornado disasters commonly unfold at the local scale and lead to fatalities due to the combination of
480 a significant (EF2+) or violent (EF4+) tornado intersecting vulnerable MH residents; and 2) demonstrate
481 how fine-scale built-environment, LULC data, Doppler radar products, and rapid post-tornado forensic
482 assessments can be combined to better understand tornado impacts, specifically regarding fatalities. A
483 bulleted list of conclusions is provided below:

- 484 • The Beaugard-Smith Station, AL tornado is representative of tornado disasters in the Southeast
485 U.S. where the intersection of a significant or violent tornado with MH structures leads to a high
486 number of fatalities despite impacting a relatively small number of buildings (e.g., Ashley 2007;
487 Strader and Ashley 2018).
- 488 • Higher fatality rates were observed in MHs (specifically manufactured homes) when compared to
489 PHs. All (19 of 23) MH fatalities occurred in manufactured homes built after 1983, and 15 of the
490 19 MH fatalities occurred in manufactured homes built after 1994. Although this is just one
491 tornado event, it provides further evidence that although all of these structures were built after the
492 post-1976 HUD construction changes, and 75% after the 1994 HUD changes, they were still more
493 vulnerable compared to PHs in the same region due to the minimal wind design requirements for
494 homes located in HUD Wind Zone I.
- 495 • The fatality rate in the Beaugard-Smith Station, AL tornado was seven times greater than that of
496 the 2011 Joplin, MO EF5 tornado. This greater fatality rate is at least in part attributed to the
497 much larger percentage of MHs in the Beaugard-Smith Station, AL tornado damage path
498 compared to that of the Joplin, MO tornado.
- 499 • All homes (MHs and PHs) where fatalities occurred and anchorage systems could be ascertained
500 either entirely lacked positive anchorage to resist wind uplift forces beyond the self-weight of the
501 home, or in the case of MHs with tie-down straps and ground anchors, had what minimal positive
502 anchorage was present compromised by corrosion and other installation defects.

503 Ash et al. (2020) indicates that most MH residents in the Southeast U.S. shelter inside their home
504 during tornado events. Results from this study illustrate the potential consequences that come with this
505 decision when a tornado strikes. Thus, although SPC and NWS forecast products in the days, hours, and
506 minutes leading up to the event may have adequately communicated the tornado threat, the combination
507 of MH residents sheltering in their homes and their housing structures failing at the base of the
508 superstructure (i.e., ground anchoring) ultimately led to high number of MH fatalities. Accordingly, this
509 event seems to be an exemplar of the larger Southeast MH-tornado problem. Southeast U.S. While neither
510 PHs or MHs are built to withstand violent tornado wind speeds (+166 mph), MHs observed in our study
511 demonstrate a fatal flaw in that 1) anchorage is consistently the weakest link in the structural load path for
512 HUD-compliant, Zone I MHs; and 2) anchorage failures in these MHs are often brittle due to either the
513 complete lack of positive uplift resistance in pan anchorage systems, or compromised resistance in tie-
514 down strap systems due to corrosion and improper installation. This mismatch between how MH residents
515 expect their housing structures to perform and the compromised structural systems that exist creates a
516 volatile and deadly scenario for a majority of MH residents in the Southeast U.S.

517 Southeastern U.S. states that frequently experience fatal tornado events involving MHs (Strader
518 and Ashley 2018), should consider implementing more stringent MH structural anchoring requirements
519 for newly purchased and existing MHs. At the very least, results from this study should serve to initiate a
520 dialogue among stakeholder, elected officials, emergency managers, and the public about the possibility of
521 implementing programs or strategies aimed at improving MH structural resilience through the amendment
522 of MH anchoring requirements. Currently, a large majority of MHs located in tornado-prone U.S. regions
523 such as Alabama, Mississippi, etc. are only required to comply with HUD Zone I standards. HUD Zone I
524 standards requires MHs to withstand a maximum wind speed of 70 mph (104 mph ASCE 7-16
525 equivalent). As such, MHs with greatest odds of being struck by tornadoes often contain anchoring
526 systems (e.g., aforementioned pan system) that only resist horizontal or lateral wind forces from weak
527 EF0 and EF1 tornadoes, while solely relying on the structure's own weight to resist any vertical or

528 upward wind forces. As this study has illustrated, this type of anchoring promotes violent, unsafe failure
529 sequences during significant (EF2+) tornado winds.

530 A potential solution for improving MH structural performance during tornado events is to require
531 all MHs in tornado-prone regions to comply to HUD Zone II or III building and anchoring standards.
532 Increasing anchoring requirements up to Zone II and III levels has been shown to improve MH
533 performance during extreme winds (IBTS, 2005; Simmons and Sutter, 2008; Hebert and Levitan, 2009).
534 It is surmised that requiring similar for MHs in tornado-prone regions would also improve their structural
535 performance and resilience during tornado events and reduce the odds of fatality. Although this study
536 does not directly assess or measure the mechanisms and economic costs for bringing all tornado-prone
537 MHs up to Zone II or III requirements, our findings suggest that there is value in improving MH
538 construction and anchoring standards when it comes to tornado impacts. Retrofitting and enforcing better
539 anchoring systems for MHs would undoubtedly increase resident survivability and reduce future disaster
540 costs.

541 As intensioned, a limitation of this study is that it focuses on one tornado disaster in the
542 Southeast, and results should be extrapolated with care. Particularly with respect to the contrast in
543 vulnerability between MHs and PHs, we recognize that the vulnerability of both housing types exists on a
544 spectrum and characterizing their relative vulnerability in broad statements can overly simplify more
545 nuanced issues. For example, our study has highlighted that there are some PHs that can perform similarly
546 to MHs due to a complete lack of positive anchorage. Nevertheless, prior research (e.g., Ashley 2007;
547 Sutter and Simmons 2010; Strader and Ashley 2018) has repeatedly demonstrated that the Southeast U.S.
548 does indeed suffer from a tornado-MH problem that leads to a disproportionate number of MH residents
549 killed in tornado events. Results presented herein point to the need for future work aimed at targeted
550 assessments of MH structural performance during tornado events. Additional research that includes more
551 thoroughly investigating the relationships that exist among tornado wind speeds, structural response
552 beyond structural design wind speeds, MH construction and anchorage installation practices (particularly
553 the impacts of increased use of pan systems), fatalities, and survivability factors is also needed.

554 Subsequent research by the authors will investigate and explore potential engineering mitigation strategies
555 that may bolster MH resident safety during tornado events. Forthcoming research will also examine this
556 issue from a cost-benefit standpoint so that recommendations to MH manufacturers, wholesale dealers,
557 installers, and homeowners can be provided, reducing losses.

558 Findings and methodologies applied in this study should be used to further NWS Integrated
559 Warning Teams' (IWT; i.e., forecasters, emergency manager, media partners, and engineers) and the
560 general public's understanding of how tornado disasters take place. By improving tornado disaster
561 knowledge, education, and assessment techniques, mitigation and resilience-building strategies can be
562 developed and employed by local, state, and federal entities. Future consideration should be given to
563 tornado events that intersect localized area of low-income populations where residents often live in MHs.
564 Historically, the total financial cost on the underlying population and built-environment for many of these
565 Southeast tornado-MH events does not meet the minimum requirements for federal support or disaster
566 recovery (Pacific Standard 2019). In addition, MH residents are less likely to have insurance to assist
567 them in recovery (Talkpovert.org 2019). These issues together exacerbate MH resident inequalities and
568 result in long-lasting impacts to tornado disaster victims. In all, lines of communication should be opened
569 between decision makers (e.g., Federal Emergency Management Agency (FEMA), emergency managers,
570 elected officials, policy makers) and members of the manufactured housing industry. These groups must
571 work together to improve resident survivability and ensure the safety of MH residents not only in the
572 Southeast. U.S., but in all tornado-prone regions throughout the country.

573 **Data Availability**

574 Some data generated or used during the study are proprietary or confidential in nature and may
575 only be provided with restrictions (e.g., mobile/manufactured housing location data, and the precise
576 fatality data). All other data are made available upon request or publicly available.

577 **Acknowledgements**

578 This research was supported by the National Oceanic and Atmospheric Administration (NOAA)
579 Verifications of the Origins of Rotation Experiment in the Southeast (VORTEX-SE) grant numbers
580 NA17OAR4590191 and NA19OAR4590213. Additional support was provided by the National Science
581 Foundation under award number CMMI 18-41667, which formed the Structural Extreme Events
582 Reconnaissance (StEER) network. Contributions from StEER and its members are acknowledged and
583 appreciated, as well as Tim Marshall and Martin Montgomery, who also conducted on-site assessments
584 and shared data and insights. Lastly, we would like to thank the anonymous reviewers for their thorough
585 feedback, comments, and suggestions.

586 **References**

- 587 Ash, K. D. 2017. "A qualitative study of mobile home resident perspectives on tornadoes and tornado
588 protective actions in South Carolina, USA." *GeoJournal*, 82 (3), 533-552.
- 589 Ash, K. D., M. J. Egnoto, S. M. Strader, W. S., Ashley, D. B. Roueche, K. E. Klockow-McClain, D.
590 Caplen, and M. Dickerson. 2020. "Structural forces. Perception and vulnerability for tornado
591 sheltering within mobile and manufactured housing in Alabama and Mississippi, USA." *Weather,
592 climate, and society*. <https://doi.org/10.1175/WCAS-D-19-0088.1>
- 593 Ashley, W. S. 2007. "Spatial and temporal analysis of tornado fatalities in the United States: 1880–2005."
594 *Weather and forecasting*, 22 (6), 1214-1228.
- 595 Ashley, W. S. and S. M. Strader. 2016. "Recipe for disaster: How the dynamic ingredients of risk and
596 exposure are changing the tornado disaster landscape." *Bulletin of the American Meteorological
597 Society*, 97 (5), 767-786.
- 598 Bodine, D. J., M. R. Kumjian, R. D. Palmer, P. L. Heinselman, and A. V. Ryzhkov. 2013. "Tornado
599 damage estimation using polarimetric radar." *Weather and forecasting*, 28 (1), 139-158.
- 600 Brooks, H. E. and J. Correia Jr. 2018. "Long-term performance metrics for National Weather Service
601 tornado warnings." *Weather and forecasting*, 33 (6), 1501-1511.

602 Burgess, D., K. Ortega, G. Stumpf, G. Garfield, C. Karstens, T. Meyer, B. Smith, D. Speheger, J. Ladue,
603 R. Smith and T. Marshall. 2014. 20 May 2013 Moore, Oklahoma, tornado: Damage survey and
604 analysis. *Weather and forecasting*, 29 (5), 1229-1237.

605 Census. 2020. *Explore Census Data*. <https://data.census.gov/cedsci/?q=mobile%20home>

606 Clarke, L. 2005. Worst-case thinking: An idea whose time has come. *Nat. Hazards Obs.*, 293, 1-3.

607 Cutter, S. L., B. J. Boruff, and W. L. Shirley. 2012. "Social vulnerability to environmental hazards." In
608 *Hazards vulnerability and environmental justice*. 143-160. Routledge.

609 Egnew, A. C., D. B. Roueche, and D. O. Prevatt. 2018. "Linking building attributes and tornado
610 vulnerability using a logistic regression model." *Natural hazards review*, 19 (4): 04018017.

611 Federal Emergency Management Agency (FEMA). 2007. *February 2007 Tornado Recovery Advisory:
612 Understanding and Improving Performance of New Manufactured Homes During High-Wind
613 Events*. FEMA DR 1679 RA5, FEMA Region IV, Atlanta, GA.

614 Federal Emergency Management Agency (FEMA). 2013. *Wind Zone Comparisons (HUD's MHCSS and
615 FEMA 85)* Accessed March 3, 2020. [https://www.fema.gov/media-library-data/20130726-1501-
616 20490-5921/fema_p85_apndx_g.pdf](https://www.fema.gov/media-library-data/20130726-1501-20490-5921/fema_p85_apndx_g.pdf)

617 Gibbs, J. G. and B. R. Bowers. 2019. "Techniques and Thresholds of Significance for Using WSR-88D
618 Velocity Data to Anticipate Significant Tornadoes." *Journal of operational meteorology*, 7 (9),
619 117-137.

620 Hebert, K. and Levitan, M., 2009, June. Performance of Manufactured Housing in Louisiana during
621 Hurricanes Katrina and Rita. In 11th American Conference on Wind Engineering, San Juan, PR.

622 Institute for Building Technology and Safety (IBTS). 2005. An Assessment of Damage to Manufactured
623 Homes Caused by Hurricane Charley." Prepared for the U.S. Department of Housing and Urban
624 Development (HUD), Washington, D.C.

625 Homeland Infrastructure Foundation-Level Data (HIFLD). 2020. *HIFLD Open Data*. [https://hifld-
626 geoplatform.opendata.arcgis.com/](https://hifld-geoplatform.opendata.arcgis.com/)

627 Kensler, C. D. (1985). The Morgan Hill earthquake of April 24, 1984—effects on mobile homes.
628 *Earthquake spectra*, 1(3), 607-613.

629 Kijewski-Correa, T., Prevatt, D., Mosalam, K., Robertson, I., and Roueche, D. 2018. Structural Extreme
630 Events Reconnaissance (StEER) Network. <https://www.steer.network/>

631 Kingfield, D. M. and J. G. LaDue. 2015. “The relationship between automated low-level velocity
632 calculations from the WSR-88D and maximum tornado intensity determined from damage
633 surveys.” *Weather and forecasting*, 30 (5), 1125-1139.

634 Kuligowski, E. D., F. T. Lombardo, L. T. Phan, M. L. Levitan, and D. P. Jorgensen. 2014. *Final report,*
635 *National Institute of Standards and Technology (NIST) technical investigation of the May 22,*
636 *2011, tornado in Joplin, Missouri* (No. National Construction Safety Team Act Reports (NIST
637 NCSTAR)-3).

638 Lombardo, F. T., D. B. Roueche, and D. O. Prevatt. 2015. “Comparison of two methods of near-surface
639 wind speed estimation in the 22 May 2011 Joplin, Missouri Tornado.” *Journal of Wind*
640 *Engineering and Industrial Aerodynamics*, 138, 87-97.

641 Marshall, T. P. (1993). Lessons learned from analyzing tornado damage. *Geophysical Monograph-*
642 *American Geophysical Union*, 79, 495-495.

643 Marshall, T. P. 2002. “Tornado damage survey at Moore, Oklahoma.” *Weather and forecasting*, 17 (3),
644 582-598.

645 McDonald, J. R. and K. C. Mehta. 2004. “A recommendation for an enhanced Fujita scale (EF-Scale).”
646 Accessed Jan 6, 2020. <https://www.spc.noaa.gov/faq/tornado/ef-ttu.pdf>

647 Microsoft US Building Footprints. 2018. “Building Footprints”. [https://www.microsoft.com/en-](https://www.microsoft.com/en-us/maps/building-footprints)
648 [us/maps/building-footprints](https://www.microsoft.com/en-us/maps/building-footprints)

649 National Centers for Environmental Information (NCEI). 2019 “Billion-Dollar Weather and Climate
650 Disasters: Summary Stats.” Accessed Jan 5, 2020. [https://www.ncdc.noaa.gov/billions/summary-](https://www.ncdc.noaa.gov/billions/summary-stats)
651 [stats](https://www.ncdc.noaa.gov/billions/summary-stats)

652 National Severe Storms Laboratory (NSSL). 2019. *Multi-Radar/Multi-Sensor System MRMS*.
653 <https://www.nssl.noaa.gov/projects/mrms/>

654 National Weather Service (NWS), KMXX Doppler Radar Site. 2019a. *East Alabama Radar*.
655 <https://radar.weather.gov/ridge/radar.php?rid=mxx&product=NOR&overlay=11101111&loop=no>

656 National Weather Service (NWS), Birmingham Weather Forecast Office (WFO). 2019b. Beauregard-
657 Smiths Station EF-4 Tornado (Macon/Lee Counties) March 3, 2019.
658 https://www.weather.gov/bmx/event_03032019beauregard

659 Pacific Standard. 2019. *After the Storm: Why mobile home owners continue to suffer more from tornado*
660 *damage*. <https://psmag.com/social-justice/tornadoes-put-mobile-home-owners-at-severe-risk>

661 Paul, B. K. and M. Stimers. 2012. "Exploring probable reasons for record fatalities: the case of 2011
662 Joplin, Missouri, Tornado." *Natural hazards*, 64 (2), 1511-1526.

663 Prevatt, D., O., Coulbourne, W., Graettinger, A., J., Pei, S., Gupta, R., and Grau, D. 2012a. Joplin,
664 Missouri, Tornado of May 22, 2011: Structural Damage Survey and Case for Tornado-Resilient
665 Building Codes, ASCE. ISBN: 978-0-7844-1250-3.

666 Prevatt, D. O., J. W. van de Lindt, E. W. Back, A. J. Graettinger, S. Pei, W. Coulbourne, R. Gupta, D.
667 James, and D. Agdas. 2012b. "Making the case for improved structural design: Tornado
668 outbreaks of 2011." *Leadership and management in engineering*, 12 (4), 254-270.

669 Rhee, D. M., and F. T. Lombardo. 2018. "Improved near-surface wind speed characterization using
670 damage patterns." *Journal of Wind Engineering and Industrial Aerodynamics*, 180, 288-297.

671 Roueche, D. B. and D. O. Prevatt. 2013. "Residential damage patterns following the 2011 Tuscaloosa, AL
672 and Joplin, MO tornadoes." *J. disaster res*, 8 (6), 1061-1067.

673 Roueche, D. B., F. T. Lombardo, and D. O. Prevatt. 2017. "Empirical approach to evaluating the tornado
674 fragility of residential structures." *Journal of structural engineering*, 143 (9): 04017123.
675 <https://ascelibrary.org/doi/10.1061/%28ASCE%29ST.1943-541X.0001854>

676 Roueche, D., T. Kijewski-Correa, D. Prevatt, B. Davis, K. Mosalam, I. Robertson, K. Turner, C. Hodges.,
677 and B. Rittelmeyer. 2019. "January 2019 tornadoes in the southeastern U.S.: Field assessment
678 team early access reconnaissance report EARR". doi:10.17603/ds2-eb6e-tr31

679 Rumbach, A., E. Sullivan, and C. Makarewicz. 2020. "Mobile home parks and disasters: understanding
680 risk to the third housing type in the United States." *Natural hazards review*, 21 (2): 05020001.
681 <https://ascelibrary.org/doi/10.1061/%28ASCE%29NH.1527-6996.0000357>

682 Simmons, K.M. and Sutter, D., 2008. Manufactured home building regulations and the February 2, 2007
683 Florida tornadoes. *Natural Hazards*, 46(3), pp.415-425.

684 Simmons, K. M. and D. Sutter, D. 2009. "False alarms, tornado warnings, and tornado casualties."
685 *Weather, climate, and society*, 1 (1), 38-53.

686 Smith, B. T., R. L. Thompson, A. R. Dean, and P. T. Marsh. 2015. "Diagnosing the conditional
687 probability of tornado damage rating using environmental and radar attributes." *Weather and*
688 *forecasting*, 30 (4), 914-932.

689 Sparks, P. R. (1985). Building damage in South Carolina caused by the tornadoes of March 28, 1984.
690 Report No.: CETS-CND-031. National Academies, Washington D.C.

691 Strader, S. M., W. Ashley, A. Irizarry, and S. Hall. 2014. "A climatology of tornado intensity
692 assessments." *Meteorological applications*, 22 (3), 513-524.

693 Strader, S. M. and W. S. Ashley. 2018. "Finescale assessment of mobile home tornado vulnerability in the
694 central and southeast United States." *Weather, climate, and society*, 10 (4), 797-812.

695 Sutter, D. and K. M. Simmons. 2010. "Tornado fatalities and mobile homes in the United States." *Natural*
696 *hazards*, 53 (1), 125-137.

697 Talk Poverty. 2019. *A record-breaking tornado season is pummeling mobile home residents.*
698 <https://talkpoverty.org/2019/07/30/tornadoes-mobile-homes-south/>

699 Theobald, D. M. 2005. "Landscape patterns of exurban growth in the USA from 1980 to 2020." *Ecology*
700 *and society*, 10 (1). <http://www.ecologyandsociety.org/vol10/iss1/art32/>

701 Thompson, R. L., B. T. Smith, J. S. Grams, A. R. Dean, J. C. Picca, A. E. Cohen, E. M. Leitman,
702 Gleason, A.M. and Marsh. 2017. "Tornado damage rating probabilities derived from WSR-88D
703 data." *Weather and forecasting*, 32 (4), 1509-1528.

704 Van Den Broeke, M. S. and S. T. Jauernic. 2014. "Spatial and Temporal Characteristics of Polarimetric
705 Tornadoic Debris Signatures." *Journal of applied meteorology and climatology*, 53 (10), 2217-
706 2231.

707 Vickery, P. J., P. F. Skerlj, J. Lin, L. A. Twisdale Jr, M. A. Young, and F. M. Lavelle. 2006. "HAZUS-
708 MH hurricane model methodology. II: Damage and loss estimation." *Natural hazards review*, 7
709 (2), 94-103.

710 Wickham, J., C. Homer, J. Vogelmann, A. McKerrow, R. Mueller, N. Herold, and J. Coulston. 2014.
711 "The multi-resolution land characteristics (MRLC) consortium—20 years of development and
712 integration of USA national land cover data." *Remote Sensing*, 6 (8), 7424-7441.

713
714
715
716
717
718
719
720
721
722
723
724
725
726
727
728
729
730
731
732
733
734
735
736
737
738
739

740 **Tables and Figures**

741

Table 1. Number of homes damaged, high-risk damaged homes, fatalities, and homes with fatalities for PH, MH (all types), MH (DWMH), MH (SWMH), and all home types. Fatality rates (fatalities per 100 damaged homes) for all damaged homes and all homes with high-risk damage are also calculated for the 2019 Beauregard-Smith Station, AL tornado.

Home Type	Homes Damaged	Homes with High-Risk Damage	Fatalities	Homes with Fatalities	Fatality Rate (per 100 damaged homes)	Fatality Rate (per 100 high-risk damaged homes)
PH	175	10	4	2	2.3	40.0
MH - All Types	156	43	19	12	12.2	44.2
MH - DWMH	106	20	12	7	11.3	60.0
MH - SWMH	50	23	7	5	14.0	30.4
All Home Types	331	53	23	14	6.9	43.4

742

743

744

745

746

747

748

749

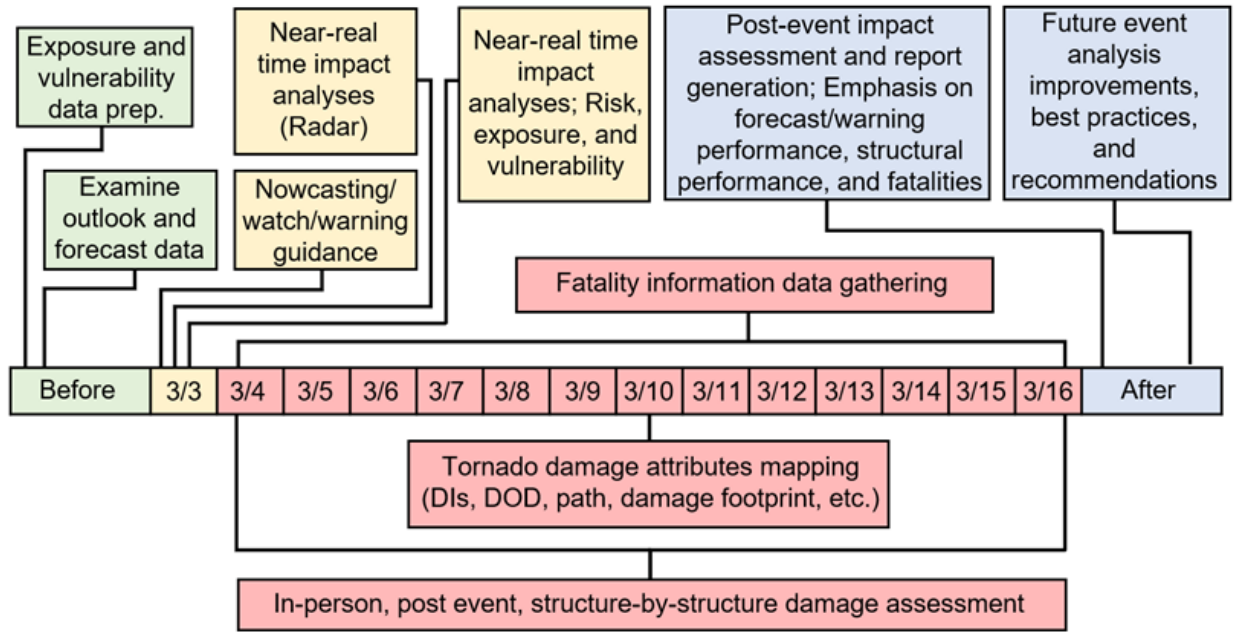
750

751

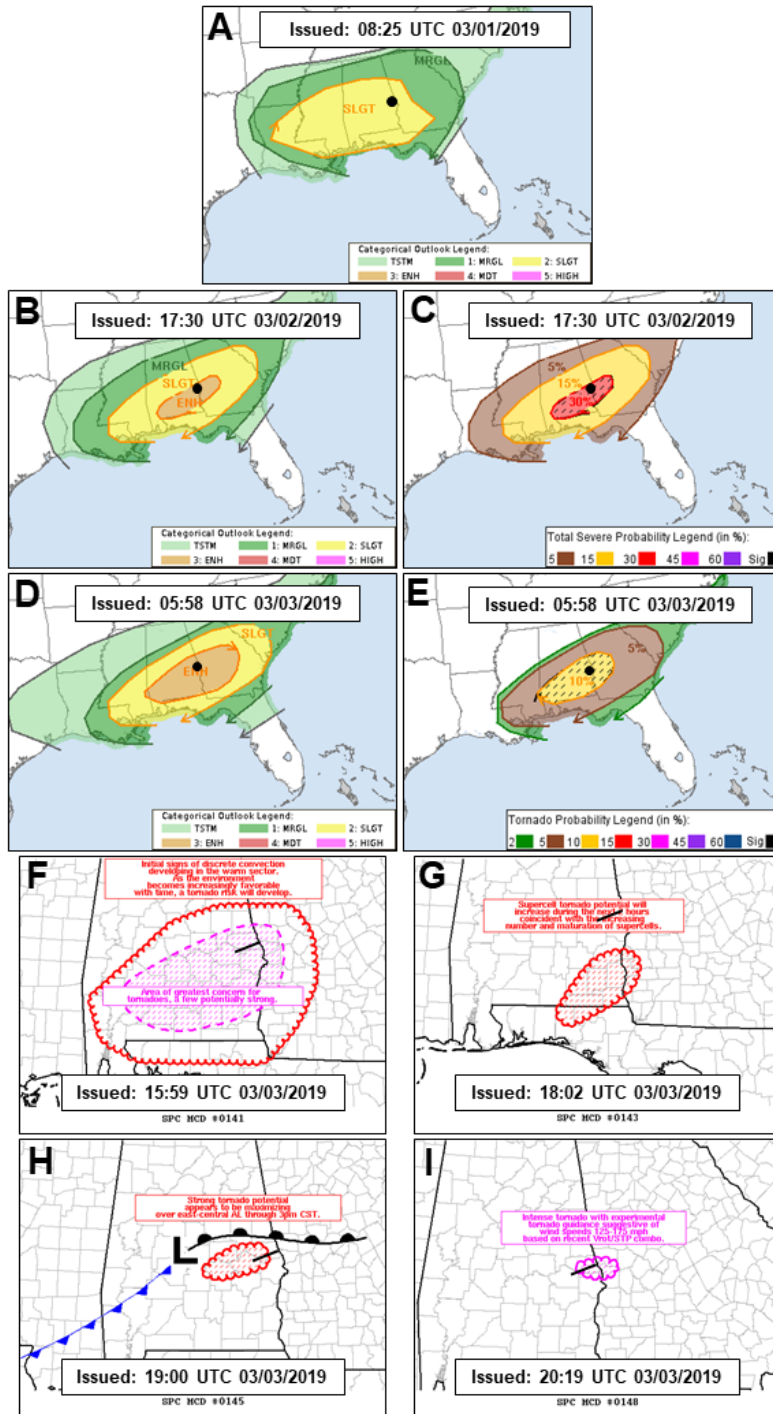
752

753

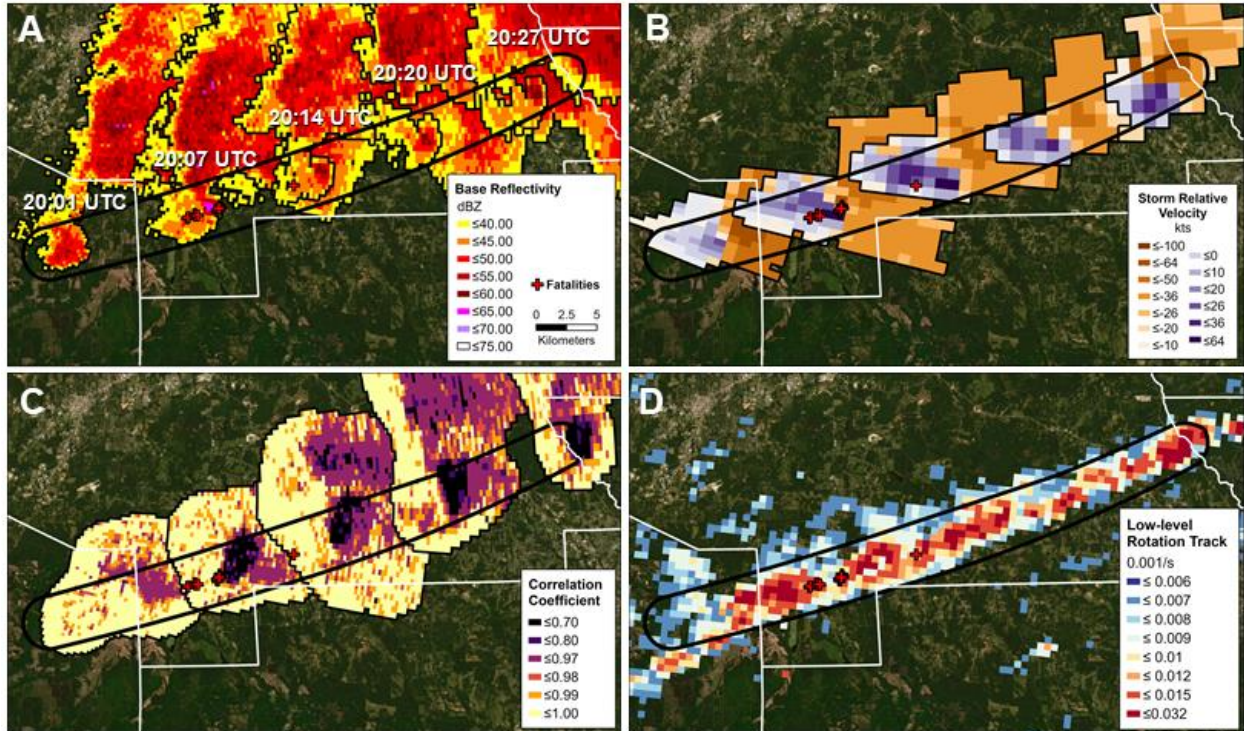
754



755
 756 **Fig. 1.** Rapid tornado impact assessment timeline example using the Beaugard-Smith Station, AL event.
 757 Green boxes represent analysis preparation steps conducted prior to the tornado event (Results Section 1);
 758 yellow boxes are near-real time analysis tasks (Results Section 2); red boxes represent post-event data
 759 gathering and assessment efforts (Results Section 3); and blue boxes indicate fatality assessments, report
 760 generation, best practices, and recommendations (Results Section 4).



761
 762 **Fig. 2.** Day 3 through Day 1 Storm Prediction Center (SPC) severe weather categorical outlooks (A, B,
 763 and D), tornado probabilities (C and E), and mesoscale discussion (MDs; F through I) for the 3 March
 764 2019 Beauregard-Smith Station tornado. A black dot represents the tornado path location in panels A
 765 through E and a black line signifies the approximate location of the tornado path in panels F through I.



766
767

Fig. 3. KMXX raw and derived radar data from 20:01 UTC to 20:27 UTC. (A) illustrates base (0.5

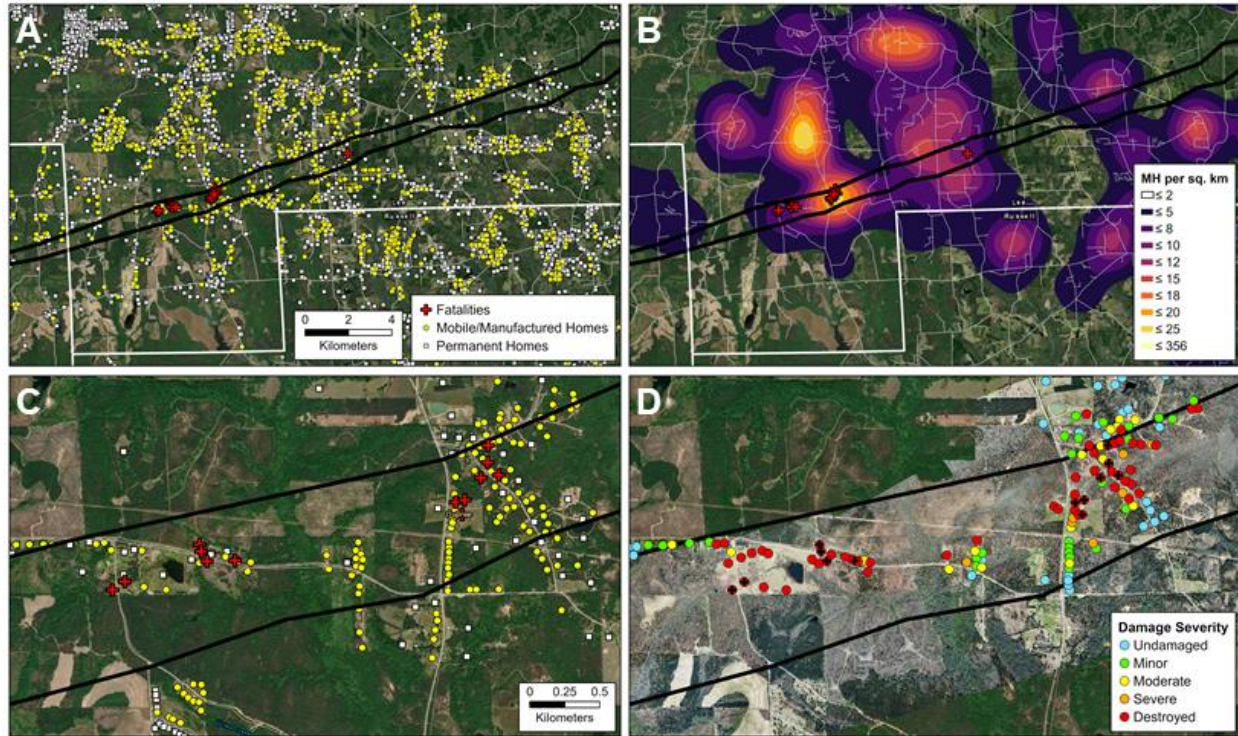
768 degrees; lowest tilt level) reflectivity (dBZ); (B) highlights base storm relative velocity (kts); (C)

769 represents the correlation coefficient scan where a tornado debris signature (TDS) was visually best

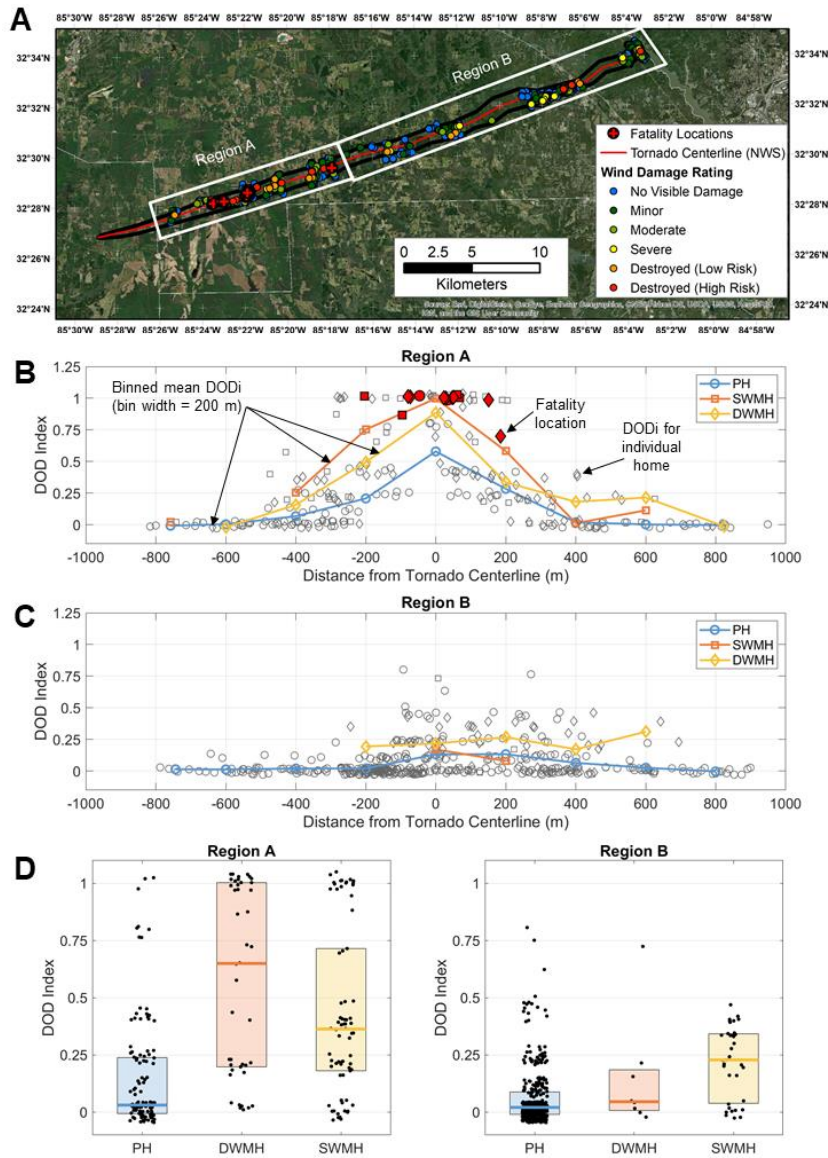
770 evident; (D) indicates the low-level rotation track (60-minute 0-2 km maximum azimuthal shear) from the

771 Multi-Radar Multi-Sensor (MRMS) project. Fatality locations are represented by red crosses and the

772 potential tornado damage area of interest (AOI) is outlined by the black polygon.

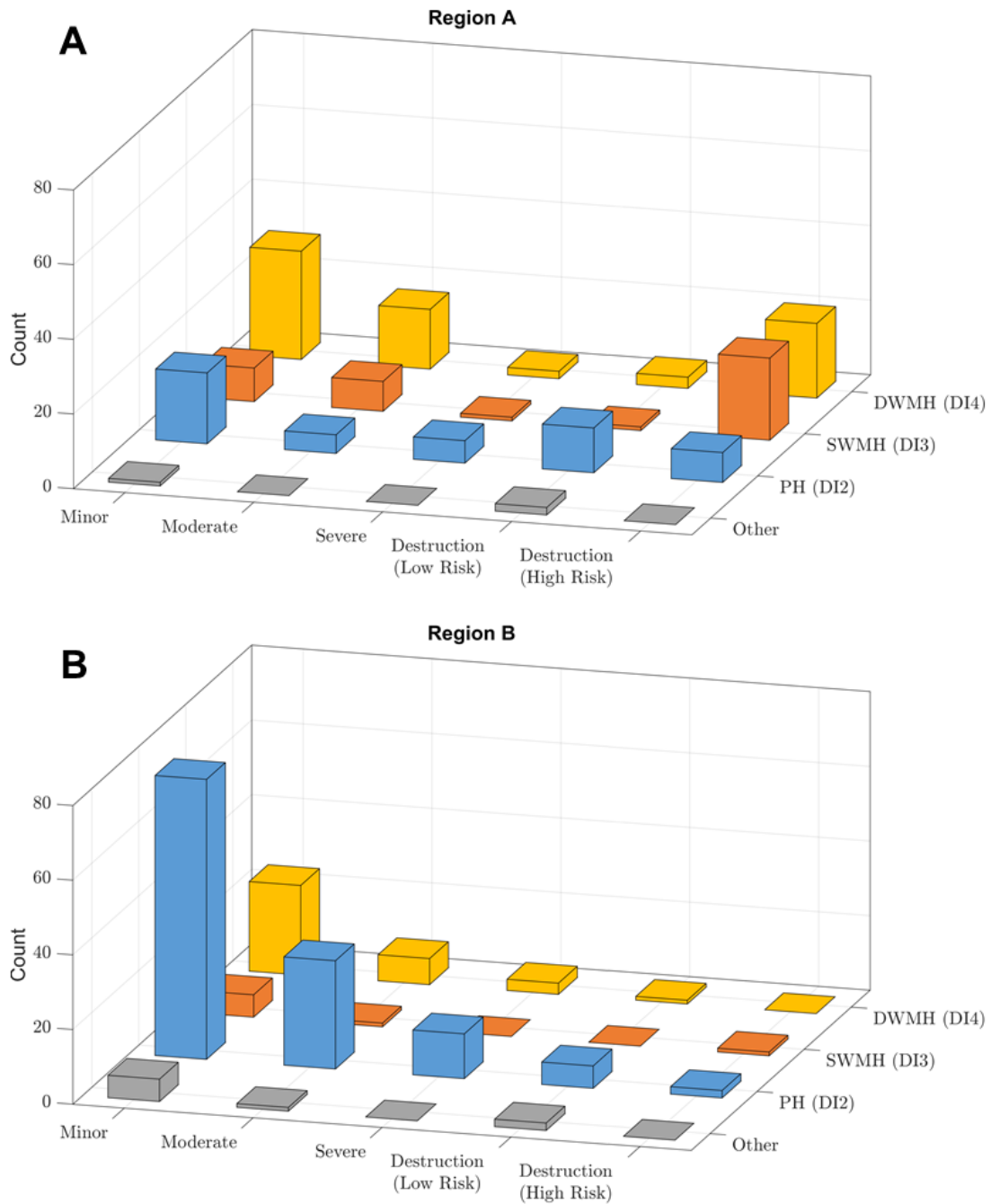


773
 774 **Fig. 4.** Beauregard-Smith Station, AL surveyed National Weather Service (NWS) tornado damage path
 775 (black outlined polygon). (A) indicates mobile/manufactured home (MH), permanent home (PH), and
 776 fatality locations (red cross); (B) illustrates MH density (MHs per km²); (C) is a zoomed in area of the
 777 Route 36 to Route 38 in Lee County, AL region where most fatalities occurred; (D) highlights the damage
 778 severity based on the post-event damage assessment.



779

780 **Fig. 5.** Wind damage assessments for all structures in the tornado path. (A) Spatial overview of entire
 781 tornado path using categorical damage ratings; (B) and (C) DODi for single-wide MHs (SWMHs),
 782 double-wide MHs (DWMHs), and permanent homes (PHs) in Region A and Region B of the tornado with
 783 respect to the center of the tornado. Lines indicate average DODi over 200 m bins. Negative distances
 784 indicate homes located on the north side of the centerline. Jitter has been added to the y-coordinates to
 785 facilitate better visualization. Red filled markers in plots (B) and (C) indicate fatality locations. (D) Box
 786 plot indicating the median, 25th and 75th percentiles of DODi for all PHs, SWMHs, and DWMHs in
 787 Regions A and B.



788

789 **Fig. 6.** Wind damage states of the affected buildings in (A) Region A and (B) Region B using Vickery et
 790 al. (2006) but modified to separate economic destruction from destruction posing a high risk to life-
 791 safety.



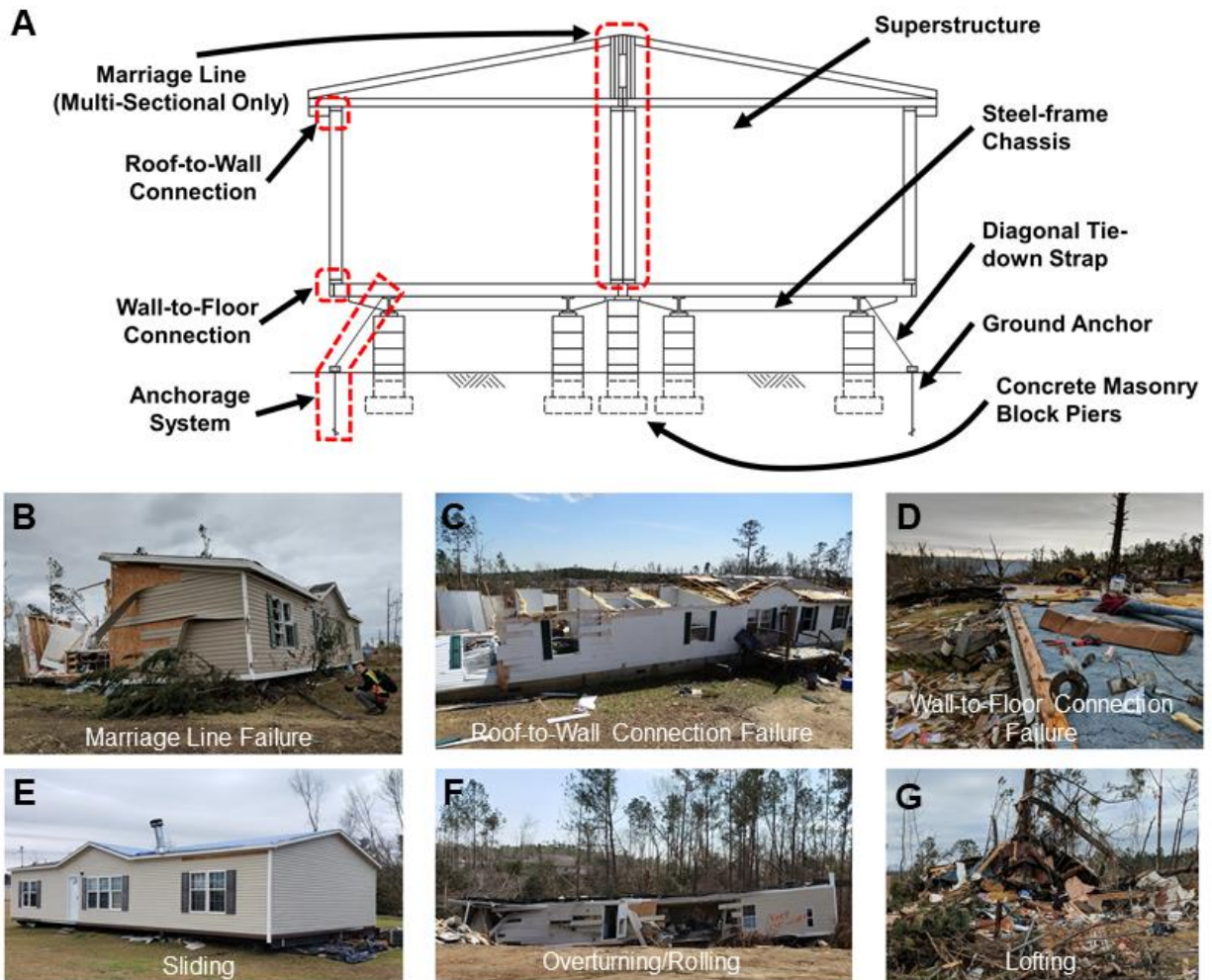
792

793 **Fig. 7.** Common anchorage problems encountered in the Beauregard, AL tornado included frequent use of

794 pan-style alternative anchorage systems – (A) and (B) – which provide no uplift resistance, and (C)

795 corrosion of diagonal ties and ground anchors. Panel B is an overturned MH with a pan anchorage system

796 illustrated (yellow circle).



797

798 **Fig. 8.** Double-wide MH (DWMH) construction diagram with critical components and their locations
 799 labeled. Red dash lines highlight those areas where common failure mechanisms occur during tornado
 800 events and relate to the below damage survey photos (Panels B-G). Failure mechanisms in MHs included
 801 (B) separation at the marriage line in DWMHs; (C) roof-to-wall connection failures; (D) wall-to-floor
 802 connection failures; and (E)-(F) failures of the anchorage system, specifically (E) sliding; (F)
 803 overturning/rolling; and (G) lofting.

804

805

806

807